Colloids and Surfaces A 579 (2019) 123634

Contents lists available at ScienceDirect

Colloids and Surfaces A

journal homepage: www.elsevier.com/locate/colsurfa

Fluorescence enhancement induced by the interaction of silver nanoclusters with lead ions in water

L. Burratti[a,*], E. Ciotta[a], E. Bolli[b], S. Kaciulis[b], M. Casalboni[a], F. De Matteis[a], A. Garzón-Manjón[c], C. Scheu[c], R. Pizzoferrato[a], P. Prosposito[a,*]

[a] Department of Industrial Engineering and INSTM, University of Rome Tor Vergata, Via del Politecnico 1, Rome, 00133, Italy
[b] Institute for the Study of Nanostructured Materials, CNR of Italy, Monterotondo Stazione, 00015, Rome, Italy
[c] Max-Planck-Institut für Eisenforschung GmbH, Max-Planck-Straße 1, 40237, Düsseldorf, Germany

GRAPHICAL ABSTRACT

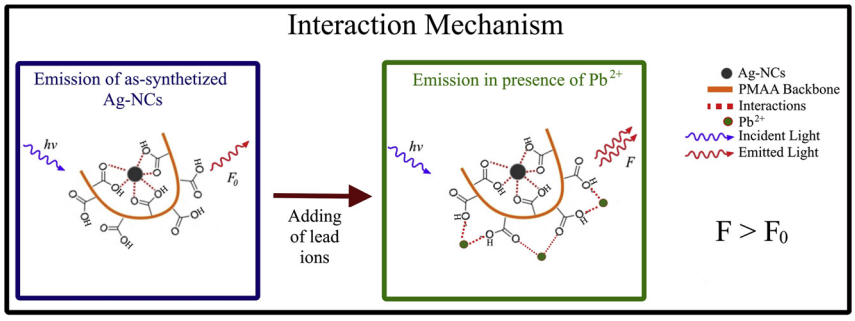

ARTICLE INFO

Keywords:
Silver nanoclusters
Photoluminescence
Fluorescence enhancement
Optical detection
Heavy metal ions
Environmental applications

ABSTRACT

We have synthesized fluorescent and stable silver nanoclusters (AgNCs) capped with poly (methacrylic acid), PMAA, by UV irradiation process. The NCs are well dispersed in aqueous solution and present a uniform distribution with an average dimension of 1.45 ± 0.26 nm. The fluorescence excited at 340 nm was found to be sensitive to the presence of heavy metal ions in solution. In particular, a peculiar fluorescence enhancement was detected upon interaction with lead(II) ions. A linear behavior of the fluorescence intensity as a function of the Pb^{2+} concentration was measured and a detection limit of 60 nM was estimated. A possible mechanism of the interaction between AgNCs and metal ions is discussed.

1. Introduction

Metal nanoparticles (MNPs) and metal nanoclusters (MNCs) have been extensively studied in recent years for their ability to sense the presence of different contaminants in water [1–3]. In many cases, the sensing process is based on a change of the optical properties in the presence of the specific contaminant. MNPs, with dimensions in the range from few nanometers to some tens of nanometers, present a typical intense and well-shaped optical absorption band, usually in the visible spectral region, due to localized surface plasmon resonance (LSPR), with no radiative emission [4,5]. Differently, MNCs show a noticeable fluorescent emission due to their extremely small dimensions giving rise to discrete energy levels [6–11]. The sensitivity of the fluorescence to the external environment is usually very high and, for this reason, MNCs have recently been investigated for sensing applications [12–14].

* Corresponding authors.
E-mail addresses: luca.burratti@uniroma2.it (L. Burratti), paolo.prosposito@uniroma2.it (P. Prosposito).

https://doi.org/10.1016/j.colsurfa.2019.123634
Received 28 May 2019; Accepted 1 July 2019
Available online 09 July 2019
0927-7757/

A huge variety of contaminants can be detected by optical methods, ranging from organic [15–18] to inorganic ones [19,20]. Among inorganic contaminants, heavy metal ions are quite common in the environment, due to the natural presence in the earth's crust, but also, to the intensive industrial processes. Some of them can cause serious disease and poisoning. Lead (Pb), for instance, can adversely affect many human organs such as kidneys, the nervous, immune, reproductive and cardiovascular systems [21,22]. Cadmium (Cd) is carcinogenic by the inhalation route, but not by the oral route [23]. Zinc (Zn) is an essential component for many physiological functions such as normal immune function or neurosensory, however high-dose can be dangerous.

In order to detect heavy metal ions in samples, several techniques based on sophisticated and expensive instrumentations are used. Among these techniques, Inductively Coupled Plasma-Atomic Emission Spectroscopy (ICP-AES) [24], Cold Vapor-Atomic Absorption Spectrophotometry (CVAAS) [25] and Atomic Fluorescence Spectroscopy (AFS) [26] are the most used and accurate to determine chemical species in an unknown sample. On the other hand, these methods need well-trained operators, proper samples preparation and are usually time-consuming. Finding low cost and easy-to-use procedures for the detection of contaminants in water is therefore a challenge. A possible route could be represented by optical sensors based on changes of the optical properties such as absorption or fluorescence; these have already been used successfully to detect several types of contaminants such as biological species [27–29] and heavy metal ions [30–32]. In particular, MNCs based on gold (Au), silver (Ag), copper (Cu) and platinum (Pt) have widely been suggested [33–40] for heavy metal ion detection.

Various types of chemical ligands can be exploited to stabilize MNCs in solution, such as small molecules [41,42], polymers [43,44] or DNA strands [45,46]. If properly functionalized, MNCs can be selective only to one or two heavy metal ion contaminants [35,47].

In this paper, we report on a facile photochemical synthesis of silver nanoclusters (AgNCs) stabilized with the polymer polymethacrylic acid (PMAA) based on UV irradiation. The optical characterization shows an absorption feature at 420 nm and a fluorescence at 650 nm indicating quantum confinement of the Ag electrons in the small nanoclusters. The size distribution and morphology of the AgNCs were determined by High Resolution Transmission Electron Microscopy (HRTEM). In addition, we studied the AgNCs fluorescence behavior in the presence of several heavy metal ions and found a marked sensitivity to some of the ions, but mainly to lead(II), which produced a strong fluorescence enhancement progressively increasing with the ion concentration. A discussion of the possible interaction mechanism between AgNCs and Pb^{2+} ions is presented.

2. Materials and methods

2.1. Chemicals and reagents

Silver nitrate ($AgNO_3$), polymethacrylic acid sodium salt solution (PMAA at a concentration of 30% in wt, Mw = 9500), sodium hydroxide (NaOH) and nitric acid (HNO_3) were purchased from Sigma Aldrich and were used as received without further purification. We tested the response of our optical device to several metal ions. Some of them were in form of nitrates, such as copper nitrate pentahydrate [$Cu(NO_3)_2{\cdot}5H_2O$], lead nitrate [$Pb(NO_3)_2$], zinc nitrate hexahydrate [$Zn(NO_3)_2{\cdot}6H_2O$], cadmium nitrate pentahydrate [$Cd(NO_3)_2{\cdot}5H_2O$]. Some other ion salts were chlorides, such as nickel chloride hexahydrate [$NiCl_2{\cdot}6H_2O$], cobalt chloride hexahydrate [$CoCl_2{\cdot}6H_2O$], potassium perchlorate [$KClO_4$], magnesium perchlorate [$Mg(ClO_4)_2$] and sodium chloride [NaCl]. We also tested the sensitivity to As(III) using sodium (meta)arsenite [$NaAsO_2$]. All reagents were dissolved in deionized water (MilliQ water).

2.2. Synthesis of silver nanoclusters

Silver nanoclusters were synthesized starting from an $AgNO_3$ water solution with a concentration of 50 mM and PMAA as capping agent with a relative concentration chosen to have a molar ratio of carboxyl groups to Ag^+ ions equal to 1:2, in order to maximize the fluorescence emission [43,48]. The Ag^+ solution was mixed with the PMAA solution and the pH was adjusted to 4.5 by adding HNO_3. The proper pH value helps the interaction between Ag^+ ions and carboxyl ($-COOH$) groups, giving the right structural conformation to polymer chains and avoiding the aggregation of AgNCs. As a final step, the mixture was exposed to UV lamp (300 W, NEWPORT, Oriel Instruments, U.S.A.) for 6 min to promote the reduction reaction of silver ions to silver metal [48,49]. The best duration time of UV exposure was optimized through an analysis of the fluorescence intensity. After 6 min we obtained the highest fluorescence emission. Nitrogen gas was fluxed on the solution surface during all the UV exposition to hamper the oxidation of the growing AgNCs.

An ultracentrifugation process (two steps of 15 min at T = 4 °C: the first one at 50,000 *g* and the second one at 100,000 *g*, OPTIMA MAX XP, Beckman Coulter, U.S.A) was applied to the solution to increase the monodispersity of the AgNCs. Only the supernatant solution was collected and subsequently used for the characterization and the measurements. The final solution was kept in the dark at T = 4 °C, before use in the sensitivity measurements. The AgNCs system resulted stable as a function of time. Both the absorbance and the fluorescence were measured every two days for two months after the synthesis and no differences were detected, indicating a high stability of the system.

2.3. Characterization of silver nanoclusters

We have characterized the AgNCs solutions by optical absorption and fluorescence spectroscopy. Absorption spectra were recorded with a Perkin-Elmer Lambda 19 spectrometer in the range of 300–700 nm. The photoluminescence (PL) emission of our AgNCs was collected by a typical photoluminescence apparatus with a 90-degree geometry, equipped with a Hg(Xe) discharge lamp (Orel instruments, Stratford, CT, USA) an excitation 25-cm monochromator (Photon Technology International, INC., Birmingham NJ, USA), an emission 25-cm monochromator (Cornerstone 260, Stratford, CT, USA) with proper excitation-rejection filters and a R3896 photomultiplier (Hamamatsu Photonics Corp., Bridgewater, NJ, USA) for the detection [50,51].

Furthermore, HRTEM technique has been used in order to analyze the morphology, size and shape of the AgNCs. The HRTEM characterization of AgNCs was carried out in a TEM equipped with an image corrector (FEI Titan Themis 60–300 X-FEG) operated at 300 kV. TEM images were recorded with 4 k x 4 k pixels on a metal-oxide-semiconductor (CMOS) camera.

X-ray Photoemission Spectroscopy (XPS) investigations have been carried out in an Escalab MkII (VG Scientific Ltd., East Grinstead, UK) spectrometer, equipped with a standard Al Kα excitation source and a five-channeltron detection system. The photoemission spectra were collected at 50 eV pass energy of the analyzer in small-area mode A3 × 8 of electrostatic lens with a diameter of about 1 mm. Spectroscopic data have been acquired and processed by using Avantage v.5 software (Thermo Fisher Scientific Ltd., East Grinstead, UK).

2.4. Detection of heavy metal ions

In order to investigate the optical response of the system in the presence of heavy metal ion contaminants, we performed steady-state fluorescence measurements by recording the emission spectra before and after the addition of specific amounts of metal ions solution. Due to the experimental set up geometry, to prevent the inner-filter effect due to self-absorption of the AgNCs solution, we diluted the liquid samples

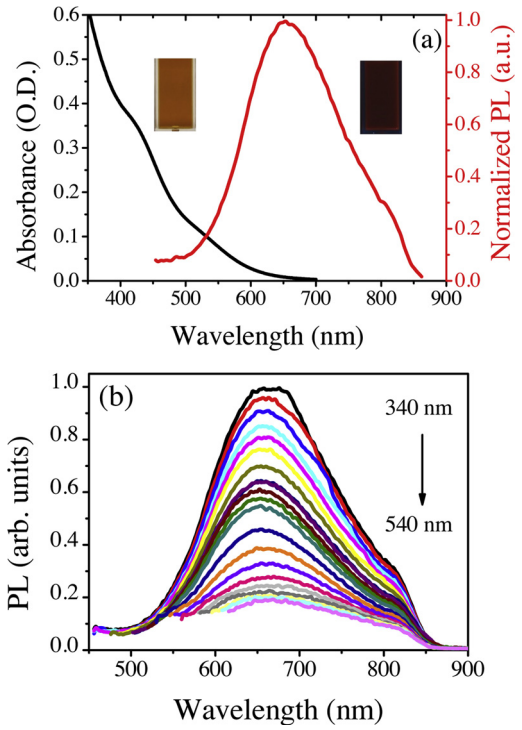

Fig. 1. Optical properties of AgNCs solution: (a) black line is the optical absorption and red curve represents the PL emission spectrum; (b) excitation spectrum of AgNCs (For interpretation of the references to colour in this figure legend, the reader is referred to the web version of this article).

20 times with respect to the initial synthesis concentration, maintaining the same pH value. The adopted procedure for the detection of ions in solution was the following. The initial reference signal of the AgNCs solution was collected without any metal ions, then the specific concentration of heavy metal ions was added and the fluorescence spectrum was measured again after five minutes. We tested several heavy metal ions such as: As(III), Cd(II), Co(II), Cu(II), K(I), Mg(II), Na(I), Ni (II), Pb(II) and Zn(II).

3. Results and discussions

3.1. Optical and structural characterizations of Ag-NCs system

Fig. 1(a) displays the absorption and fluorescence spectra of AgNCs solution in the 300–900 nm spectral range. The absorption presents a clear shoulder at 420 nm and a smaller shoulder at around 520 nm (black curve in Fig. 1). The fluorescence spectrum (red curve in figure) shows a maximum at 650 nm when excited with a 340 nm wavelength. The insets in Fig. 1 represent the photograph under white light (left side) and UV light (right side), respectively. Fig. 1(b) shows the excitation spectra of AgNCs using different excitation wavelengths from 340 to 540 nm. The emission shape and the peak wavelength remain the same for all the excitation wavelengths, while the peak intensity decreases with increasing excitation wavelength. This behavior is an indication of the good monodispersity of the AgNCs since different sizes of the clusters would produce different fluorescence profiles, as reported in the literature [43,48,52]. We performed quantum yield (QY) measurement, obtaining a value of 0.2%, using Rhodamine B as reference.

By using HRTEM microscopy, we investigated the morphology of AgNCs. In particular, this technique confirmed that ultracentrifugation was effective in separating small nanoclusters from bigger nanoclusters and aggregates. Fig. 2(a) displays HRTEM image of the bottom part of the AgNCs solution after ultracentrifugation, showing the presence of

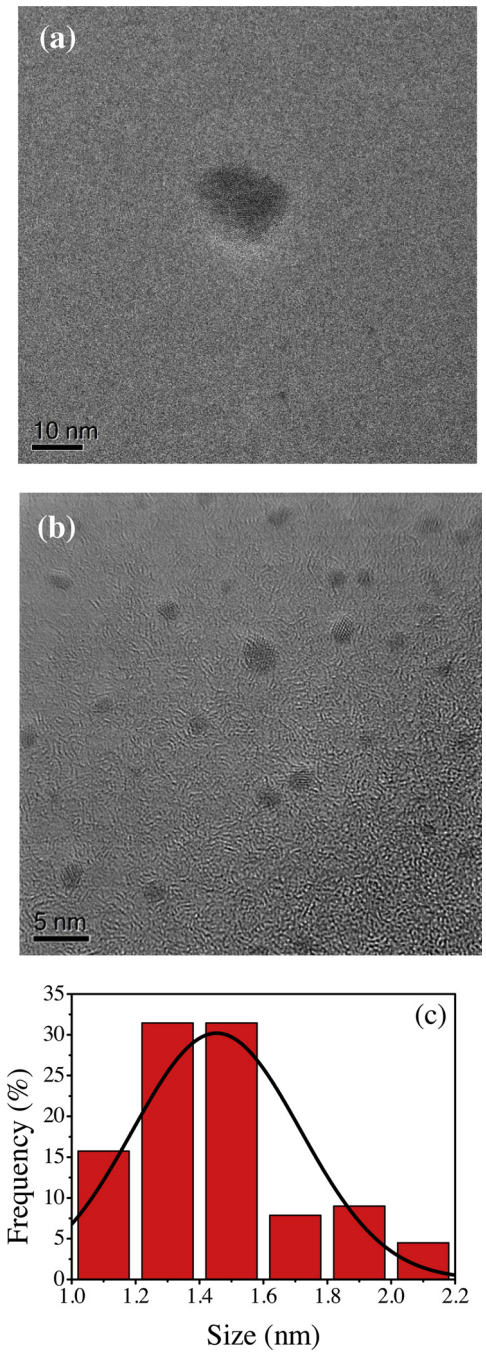

Fig. 2. HRTEM image of an aggregate present in the bottom solution after the ultracentrifugation process (a) and of the supernatant solution (b). Size distribution obtained by a statistical analysis on 140 nanoclusters (c).

relatively large aggregates with dimensions of the order of 15–20 nm. Differently, Fig. 2(b) displays a HRTEM image of the supernatant solution after the ultracentrifugation process. In this case, the AgNCs appear to be well dispersed on the entire area with no aggregates and a uniform distribution of their sizes. By a statistical analysis on 140 nanoclusters the size distribution was estimated to be 1.45 ± 0.26 nm. The results are shown in Fig. 2(c). The HRTEM image of a single AgNC is shown in Fig. 3. The ordered lattice of the silver atoms can be clearly distinguished as well as the facetted shape of the nanocluster. The crystalline structure is clearly visible and the lattice parameter resulted to be face centered cubic (FCC) {111} (d = 0.235 nm) [53,54].

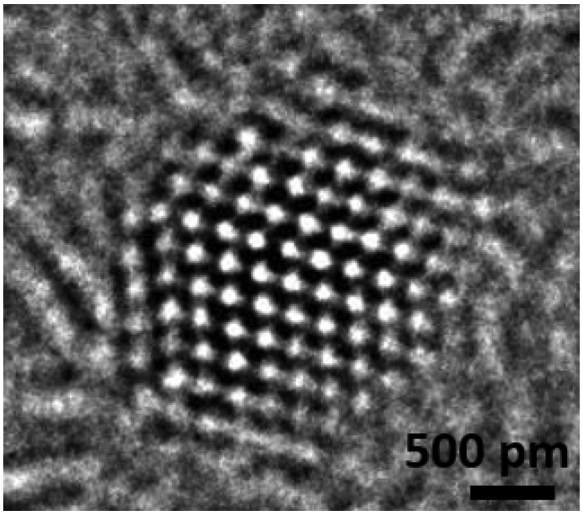

Fig. 3. HRTEM image of a single silver nanocluster.

3.2. Optical response to heavy metal ions

After the optical characterization of the pristine colloidal system, we performed optical measurements in the presence of several heavy metal ions. Absorption spectra (not shown here) did not present any substantial difference with respect to the uncontaminated solution. Such a behavior is justified by the very low absorption of the solutions due to the high grade of dilution performed to avoid self-absorption processes during the fluorescence measurements. On the contrary, fluorescence measurements showed a strong dependence on the type of contaminating heavy metal ion. The ratio of the fluorescence intensity in the presence of metal contamination (F) to that of the reference pristine solution (F_0) is shown in Fig. 4 for ten different heavy metal ions at a concentration of 50 μM. When the value of this ratio is below 1, the system with the contaminant species presented a lower intensity of the fluorescence with respect to the reference solution (fluorescence quenching or "turn off" effect). This behavior, taking into accounts the measurement errors, was not observed for any of the investigated ions. On the contrary, Zn^{2+}, Cd^{2+}, and especially Pb^{2+} produced a F/F_0 ratio greater than 1 (green bars in the figure) indicating a fluorescence enhancement or "turn on" effect.

Lead ions have often been reported to quench other luminescent systems [55–58]. Differently, fluorescence enhancement for AgNCs in the presence of lead ions was reported only by Zhang et al. [59] and by Wang et al. [60]. In both cases, the NCs were synthesized exploiting DNA scaffolds and the mechanism of the fluorescence enhancement was attributed to the special interaction between the ion and its complementary DNA strands. In our case, AgNCs were prepared using PMAA as capping agent and the presence of Pb^{2+} remarkably increased the fluorescence intensity by 1.9 times for a concentration of 50 μM. Therefore, we focused our investigation on the low concentration range of Pb^{2+} and the mechanism behind such a sensing behavior.

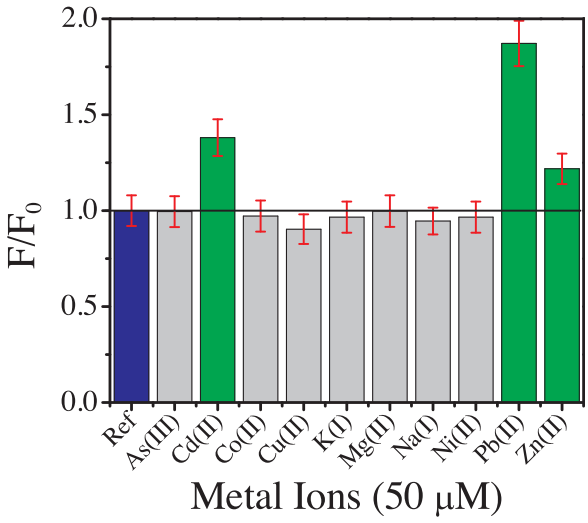

Fig. 4. Fluorescence intensity ratio of AgNCs solution in absence (F_0) and in presence (F) of various metal ions at the concentration of 50 μM.

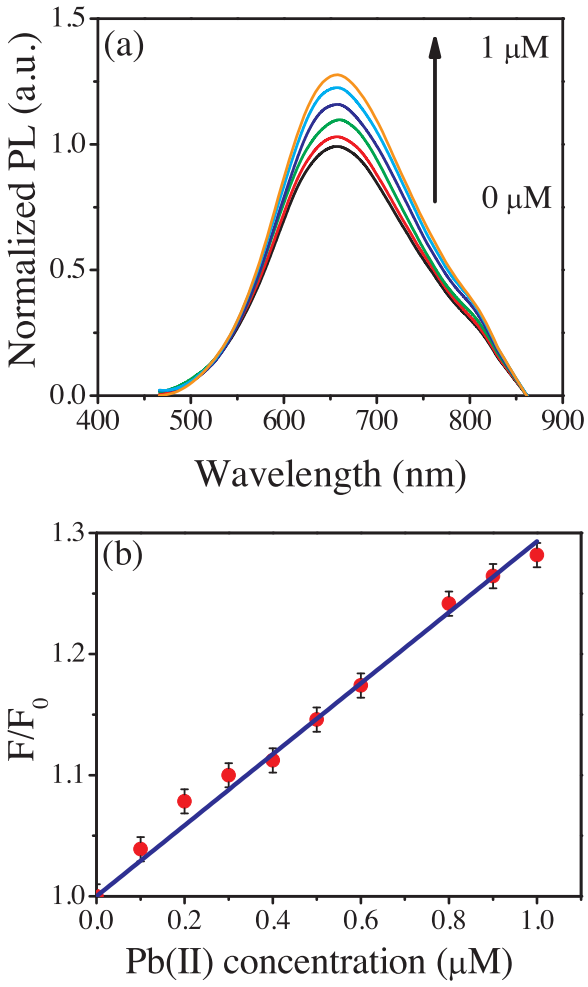

Fig. 5. (a) Fluorescence spectra of AgNCs as a function of Pb^{2+} ions concentration from 0 to 1 μM. (b) Fluorescence intensity ratio of AgNCs in the presence of Pb^{2+} ions from 0 to 1 μM. Blue line is a linear fit of the experimental points (For interpretation of the references to colour in this figure legend, the reader is referred to the web version of this article).

The fluorescence spectra of the AgNCs as a function of the lead(II) ion concentration in the range 0–1 μM are shown in Fig. 5(a), while the F/F_0 ratio is reported in Fig. 5(b). The fitting procedure of the experimental points gives a remarkable linear behavior. From the line slope, a limit of detection (LOD, 3σ) of 60 nM was estimated. It should be underlined that this value is very near to legal limit of 50 nM for drinking water established by the WHO [22]. Such a low detection limit makes our system highly interesting and worthy of being studied in more detail.

Table 1 shows the LOD and the linear range for some AgNCs systems used to detect Pb^{2+} presented in the literature. Two systems present a very good LOD, but it has to be underlined that their synthesis is quite cumbersome based on DNA strands as capping agents or on alloy of metals (Au/Ag). On the contrary, our system is very easy to prepare and presents a good LOD and a high linearity at the same time in a wide

Table 1
Comparison of AgNCs fluorescence based systems for the detection of Pb^{2+} in terms of detection limit and linear range.

AgNCs System	Limit of Detection (LOD)	Linear Behaviour	Ref Number
AgNCs - PMAA	60 nM	0 - 1000 nM	This Work
AgNCs - C-PS2.M-DNA	3 nM	0 - 500 nM	[59]
Ag/Au NCs alloy – BSA	2 nM	0 - 100 nM	[61]
Ag/Au NCs alloy – GSH	140 nM	0 - 1500 nM	[62]

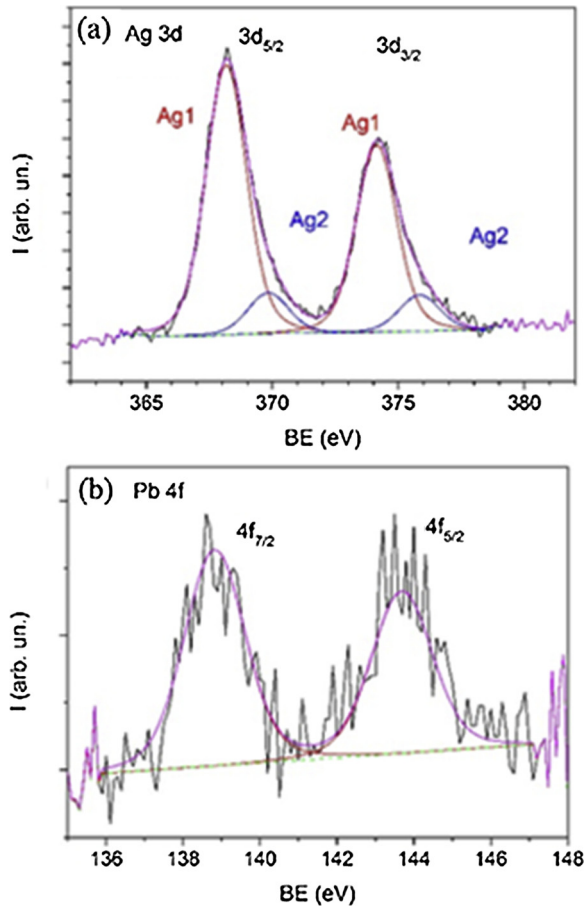

Fig. 6. XPS spectra of the regions Ag 3d (a) and Pb 4f (b).

concentration range.

3.3. Interaction mechanism between metal ions and AgNCs system

In this section, we discuss a possible interaction mechanism between the AgNCs capped with PMAA and lead ions. The XPS spectra of Ag 3d reported in Fig. 6a revealed the presence of metallic Ag (peak Ag1 at BE = 368.2 eV) and also the second peak Ag2 at BE = 369.9 eV. Since it is well-known that the chemical shift of Ag 3d is negligible [63], the peak Ag2 must be attributed to a shift of the Ag 3d position due to the reduced dimension of the silver nanoclusters, i.e. to the size-shift of Ag 3d [64,65]. It is possible to evaluate from its BE value that the size of Ag nanoclusters is less than 2 nm [64], whereas the signal of metallic state Ag1 is generated by their agglomerates, i.e. the nanoparticles bigger than about 7 nm [64]. Fig. 6b shows the spectrum of Pb 4f spin-orbit doublet for the solution after interaction with Pb^{2+} ions (concentration of 150 μM). The position of Pb $4f_{7/2}$ peak at BE = 138.8 eV indicates that the lead ions after interaction with the solution remain in their oxidation state Pb(II) rather than in the metallic state Pb(0) at BE = 136.9 eV [63]. If the lead ions interacted with silver NCs by means of strong covalent bonds, it would be possible to expect the metallic state of Pb(0). On this basis, we suggest that lead is bonded with oxygen in the carboxyl groups of the polymer chains.

In addition, no detectable difference was found between the Fourier-Transform Infrared (FTIR) spectra (not presented here) of the reference AgNCs solution and the solution after interaction with Pb^{2+}. These results are a further indication of the absence of strong covalent bonds of the lead ions neither directly with AgNCs nor with carboxyl groups present in the polymeric chains. We can instead conclude that Pb^{2+} ions could interact with −COOH groups by ion-dipole strength.

To understand the sensing behavior of AgNCs towards metal ions we referred to the mechanism of interaction between molecular fluorescent probes and metal ions. On this basis two main classes of cations fluorescent sensing processes can be distinguished [66]. The first one is based on the Photoinduced Charge Transfer (PCT) process while the second occurs through the Photoinduced Electron Transfer (PET) mechanism. Usually, PCT based sensors, after the interaction with metal ions, show a blue or red shift of the fluorescence band. Such a behavior is related to the interaction of the ion with the fluorophore, which can low or raise the molecular orbital energy levels with respect to those of the free fluorophore. Differently, for PET based sensors, the energy and shape of the fluorescence band remain unaltered in the presence of metal ions, while the intensity undergoes a strong variation that can either be a fluorescence enhancement or a fluorescence quenching, depending on the type of metal ions. The latter behavior was observed in our system. In addition, in each class of fluorescent sensors, distinctions can be made according to the structure of the complexing moiety [67]. In many cases the principle behind the turn-on sensors, where the presence of heavy metal ions induces a fluorescence enhancement, is the so called Chelation-Enhanced Fluorescence (CHEF) effect [55,68,69]. In this case the molecular fluorophore presents a weak fluorescence when the metal ions are absent since the fluorescence is quenched by PET effect. The weak fluorescence is related to the presence of the lone pair electrons of some of the fluorophore atoms or functional groups containing a lone pair of electrons having energy levels with higher energy with respect to the highest occupied molecular orbital (HOMO) of the molecular fluorophore. As consequence, after the optical excitation, the lone pair electrons can fill partially the HOMO empty states thus preventing the photo-excited electrons from returning to the HOMO state and resulting in a low fluorescence efficiency. The positive metal ions, coordinating the lone pair electrons, lower the energy level of the lone pair state below the fluorophore HOMO state thus hampering the fluorescence quenching effect and inducing an overall fluorescence enhancement [69].

In the case of the interaction of AgNCs with lead(II) ions, a similar behavior can be invoked considering a mechanism model based on PET and CHEF phenomena. Fig. 7 shows a simple representation of the AgNCs capped with PMAA with and without metal ions and the respective energy levels. In Fig. 7(a) a schematic drawing of the as-synthesized AgNCs capped with PMAA is reported. Fig. 7(b) shows the possible interaction of the system with lead ions. The black dots represent AgNCs, the orange line the polymer backbone with side carboxyl groups and the dotted red lines the interaction (ion-dipole strengths) between the clusters and carboxyl groups and between lead ions and the functional groups. The small green dots are Pb^{2+} ions. F_0 is the fluorescence induced by the optical excitation of the AgNCs without metal cations, while F is the enhanced fluorescence of the colloidal solution in presence of the contaminant.

In Fig. 7(c) and (d) the schematic drawings of the silver NCs energy levels without and with lead(II) ions are reported, respectively. In our picture, the lone pair energy level (deriving from the oxygen atoms of the carboxyl groups) has a higher energy than that of the ground state (GS) of the AgNCs. The process can be schematized as follows. The optical excitation promotes an electron from the GS to the excited state

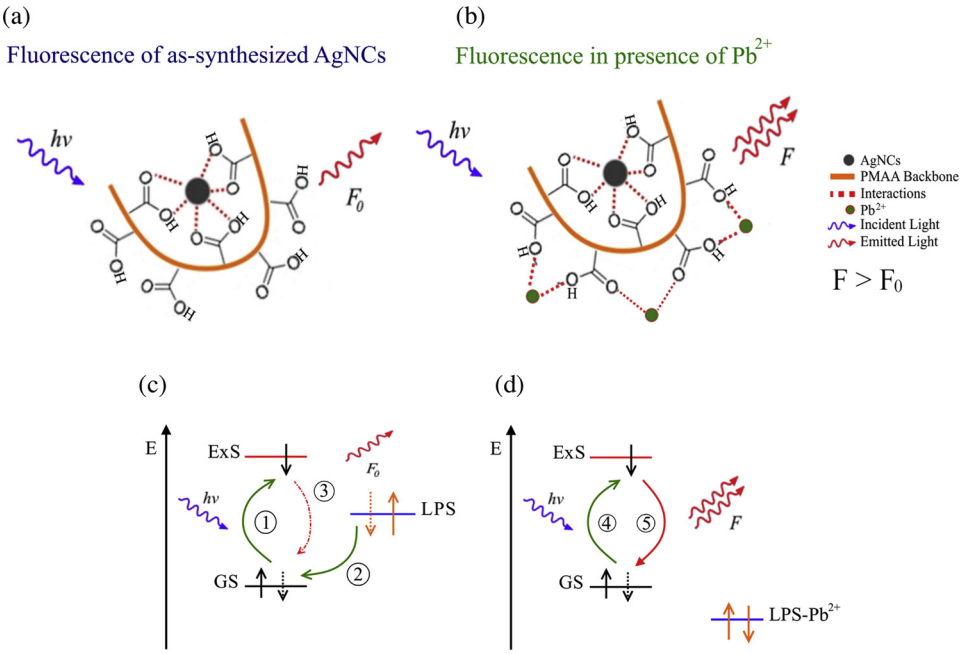

Fig. 7. Schematic drawing of the structure of AgNCs capped with PMAA (a) and the Pb^{2+} interaction with AgNCs (b). Schematic representation of electron transfers in the PET mechanism (c) and in the CHEF process (d).

(ExS) (process 1) of the AgNC as sketched in Fig. 7(c). After the optical excitation, an electron from the lone pair state (LPS) could fill the empty state left in the GS (process 2). Once the GS is filled with an electron, the radiative decay is inhibited and the fluorescence yield is low (process 3). When lead(II) ions are added to the system (Fig. 7(d)), they interact with lone pair electrons moving their energy level (LPS-Pb^{2+}) below that of the GS level of the AgNCs. In this case, the excited electron (process 4) can easily return into the GS (process 5) and the emitted fluorescence (F) is more intense than that of AgNCs without metal ions. The final result is a fluorescence enhancement dependent on the Pb^{2+} concentration as presently measured in the colloidal solutions.

The presented model is further confirmed by the time resolved fluorescence spectra (not presented here) indicating a very small increase of the average lifetime (less than 1%) in presence of the lead ions (1 μM). As expected, the inhibition of the LPS state decay channel, for some of the NCs, results in a higher fluorescence intensity but not in a substantial change of the fluorescence lifetime.

4. Conclusions

In this work, we reported a successful method to synthesize a colloidal water solution of silver nanoclusters capped with PMAA exhibiting a fluorescence at 650 nm when excited at 340 nm. By HRTEM images, we estimated an average diameter of the AgNCs equal to 1.45 ± 0.26 nm with a high degree of monodispersity. We tested the optical response of the colloidal solution to some heavy metal ions. In particular, an interesting fluorescence enhancement in the presence of Pb^{2+} was found. The fluorescence intensity showed a linear behavior as a function of the ion concentration in the range 0–1 μM with a limit of detection of 60 nM. This value is close to the legal limit of 50 nM established by WHO for drinking water. Finally, we proposed a model of interaction between the AgNCs and lead(II) ions based on the Chelation-Enhanced Fluorescence effect, which is generally assumed for the interaction of molecular fluorophores with metal ions.

Acknowledgements

The authors acknowledge the precious help of Dr. Mario Bragaglia of the Enterprise Engineering Department of the University of Rome Tor Vergata for IR measurements and Prof. Monica Bari of the Experimental Medicine Department of the University of Rome Tor Vergata for ultracentrifugal purification. Research supported by Regione Lazio through Progetto di Ricerca 85-2017-15125, founded according to L.R.13/08, and by the University of Rome Tor Vergata through the Mission Sustainability program (E86C18000450005).

References

[1] X.H. Zhang, T.Y. Zhou, X. Chen, Applications of metal nanoclusters in environmental monitoring, Chinese J. Anal. Chem. 43 (2015) 1296–1305, https://doi.org/10.1016/S1872-2040(15)60856-8.
[2] E. Oliveira, C. Núñez, H.M. Santos, J. Fernández-Lodeiro, A. Fernández-Lodeiro, J.L. Capelo, C. Lodeiro, Revisiting the use of gold and silver functionalised nanoparticles as colorimetric and fluorometric chemosensors for metal ions, Sensors Actuators, B Chem. 212 (2015) 297–328, https://doi.org/10.1016/j.snb.2015.02.026.
[3] D. Vilela, M.C. González, A. Escarpa, Sensing colorimetric approaches based on gold and silver nanoparticles aggregation: chemical creativity behind the assay, A review, Anal. Chim. Acta. 751 (2012) 24–43, https://doi.org/10.1016/j.aca.2012.08.043.
[4] F. Mochi, L. Burratti, I. Fratoddi, I. Venditti, C. Battocchio, L. Carlini, G. Iucci, M. Casalboni, F. De Matteis, S. Casciardi, S. Nappini, I. Pis, P. Prosposito, Plasmonic sensor based on interaction between silver nanoparticles and Ni2+ or Co2+ in water, Nanomater. 8 (8) (2018) 488, https://doi.org/10.3390/NANO8070488.
[5] M. Shellaiah, T. Simon, K.W. Sun, F.H. Ko, Simple bare gold nanoparticles for rapid colorimetric detection of Cr3+ions in aqueous medium with real sample applications, Sensors Actuators, B Chem. 226 (2016) 44–51, https://doi.org/10.1016/j.snb.2015.11.123.
[6] L. Maretti, P.S. Billone, Y. Liu, J.C. Scaiano, Facile photochemical synthesis and characterization of highly fluorescent silver nanoparticles, J. Am. Chem. Soc. 131 (2009) 13972–13980, https://doi.org/10.1021/ja900201k.
[7] X. Le Guével, B. Hötzer, G. Jung, K. Hollemeyer, V. Trouillet, M. Schneider, Formation of fluorescent metal (Au, Ag) nanoclusters capped in bovine serum albumin followed by fluorescence and spectroscopy, J. Phys. Chem. C. 115 (2011) 10955–10963, https://doi.org/10.1021/jp111820b.
[8] R. Jin, Atomically precise metal nanoclusters: stable sizes and optical properties, Nanoscale. 7 (2015) 1549–1565, https://doi.org/10.1039/c4nr05794e.
[9] I. Díez, M. Pusa, S. Kulmala, H. Jiang, A. Walther, A.S. Goldmann, A.H.E. Müller, O. Ikkala, R.H.A. Ras, Color tunability and electrochemiluminescence of silver nanoclusters, Angew. Chemie Int. Ed. 48 (2009) 2122–2125, https://doi.org/10.1002/anie.200806210.
[10] L. Zhang, E. Wang, Metal nanoclusters: new fluorescent probes for sensors and bioimaging, Nano Today 9 (2014) 132–157, https://doi.org/10.1016/j.nantod.2014.02.010.
[11] L. Burratti, E. Bolli, M. Casalboni, F. de Matteis, F. Mochi, R. Francini, S. Casciardi, P. Prosposito, Synthesis of fluorescent Ag nanoclusters for sensing and imaging applications, Mater. Sci. Forum. 941 (2018) 2243–2248 doi:10.4028/ www.

scientific.net/MSF.941.2243.
[12] S.T. Yang, Y. Chang, H. Wang, G. Liu, S. Chen, Y. Wang, Y. Liu, A. Cao, Folding/aggregation of graphene oxide and its application in Cu2+ removal, J. Colloid Interface Sci. 351 (2010) 122–127, https://doi.org/10.1016/j.jcis.2010.07.042.
[13] F. Wen, Y. Dong, L. Feng, S. Wang, S. Zhang, X. Zhang, Horseradish peroxidase functionalized fluorescent gold nanoclusters for hydrogen peroxide sensing, Anal. Chem. 83 (2011) 1193–1196, https://doi.org/10.1021/ac1031447.
[14] M.L. Cui, J.M. Liu, X.X. Wang, L.P. Lin, L. Jiao, Z.Y. Zheng, L.H. Zhang, S.L. Jiang, A promising gold nanocluster fluorescent sensor for the highly sensitive and selective detection of S2-, Sensors Actuators, B Chem. 188 (2013) 53–58, https://doi.org/10.1016/B978-0-7020-5193-7.00125-4.
[15] R. De Angelis, L. D'Amico, M. Casalboni, F. Hatami, W.T. Masselink, P. Prosposito, Photoluminescence sensitivity to methanol vapours of surface InP quantum dot: effect of dot size and coverage, Sensors Actuators, B Chem. 189 (2013) 113–117, https://doi.org/10.1016/j.snb.2013.01.057.
[16] S.L. Jackson, A. Rananaware, C. Rix, S.V. Bhosale, K. Latham, Highly fluorescent metal-organic framework for the sensing of volatile organic compounds, Cryst. Growth Des. 16 (2016) 3067–3071, https://doi.org/10.1021/acs.cgd.6b00428.
[17] L. Burratti, M. Casalboni, F. De Matteis, R. Pizzoferrato, P. Prosposito, Polystyrene opals responsive to methanol vapors, Materials (Basel). 11 (2018) 1547, https://doi.org/10.3390/ma11091547.
[18] L. Burratti, F. De Matteis, M. Casalboni, R. Francini, R. Pizzoferrato, P. Prosposito, Polystyrene photonic crystals as optical sensors for volatile organic compounds, Mater. Chem. Phys. 212 (2018) 274–281, https://doi.org/10.1016/j.matchemphys.2018.03.039.
[19] Y. Wu, Y. Tan, J. Wu, S. Chen, Y.Z. Chen, X. Zhou, Y. Jiang, C. Tan, Fluorescence array-based sensing of metal ions using conjugated polyelectrolytes, ACS Appl. Mater. Interfaces 7 (2015) 6882–6888, https://doi.org/10.1021/acsami.5b00587.
[20] S. Bai, C. Sun, P. Wan, C. Wang, R. Luo, Y. Li, J. Liu, X. Sun, Transparent conducting films of hierarchically nanostructured polyaniline networks on flexible substrates for high-performance gas sensors, Small 11 (2015) 306–310, https://doi.org/10.1002/smll.201401865.
[21] B. Gillis, Z. Arbieva, I. Gavin, Analysis of lead toxicity in human cells, BMC Genomics 13 (2012) 344, https://doi.org/10.1186/1471-2164-13-344.
[22] Guidelines for Drinking-water Quality: Fourth Edition Incorporating the First Addendum, World health organisation, 2017, https://doi.org/10.1016/S1462-0758(00)00006-6.
[23] R.A. Bernhoft, Cadmium toxicity and treatment, ScientificWorldJ. 2013 (2013) 394652, , https://doi.org/10.1155/2013/394652.
[24] B. Yaman, M. Yaman, Seasonal variations in concentrations of toxic trace metals in deep-sea fish, identified with stat-AAS and ICP-AES, J. Elem. 22 (2017) 127–142, https://doi.org/10.5601/jelem.2016.21.2.1117.
[25] Z.H. Fernández, L.A. Valcárcel Rojas, A.M. Álvarez, J.R. Estevez Álvarez, J. Araújo dos Santos, I.P. González, M.R. González, N.A. Macias, D.L. Sánchez, D.H. Torres, Application of Cold Vapor-Atomic Absorption (CVAAS) Spectrophotometry and Inductively Coupled Plasma-Atomic Emission Spectrometry methods for cadmium, mercury and lead analyses of fish samples. Validation of the method of CVAAS, Food Control 48 (2015) 37–42, https://doi.org/10.1016/j.foodcont.2014.05.056.
[26] F. Qu, Q. Zhang, J. You, Recognition and determination of multi-metal ions based on silver nanoclusters capped by polyethyleneimine with different molecular weights, New J. Chem. 39 (2015) 9293–9298, https://doi.org/10.1039/c5nj01867f.
[27] J. Homola, Surface plasmon resonance sensors for detection of chemical and biological species, Chem. Rev. 108 (2008) 462–493, https://doi.org/10.1021/cr068107d.
[28] F.R. Lamastra, R. De Angelis, A. Antonucci, D. Salvatori, P. Prosposito, M. Casalboni, R. Congestri, S. Melino, F. Nanni, Polymer composite random lasers based on diatom frustules as scatterers, RSC Adv. 4 (2014) 61809–61816, https://doi.org/10.1039/c4ra12519c.
[29] H.E. Katz, M.L. Schilling, W.R. Holland, T. Fang, G.D. Stucky, S.R. Marder, J.E. Sohn, R.L. Sutherland, D.G. Mclean, S. Kirkpatrick, E. Report, N. Optics, O.R. Evans, W. Lin, Y.W. Cao, X.D. Chai, S.G. Chen, Y.S. Jiang, W.S. Yang, R. Lu, Y.Z. Ren, M. Blanchard-Desce, T.J. Li, J.M. Lehn, M.C.R. Castro, A.M.C. Fonseca, M. Belsley, M.M.M. Raposo, J. a Miragliotta, N. Tsutsumi, M. Luo, Y. Song, C. Lin, N. Ye, W. Cheng, X. Long, G.S. He, L.S. Tan, Q. Zheng, P.N. Prasad, R.L. Byer, A. Avhandling, K.E.Y. Words, J. Luo, X.-H. Zhou, A.K.-Y. Jen, G.W. Watt, P. Ray, J. Byrd, A new series of nonlinear optical organic materials with molecular receptor: design and synthesis, Chem. Rev. 35 (2016) 1–18, https://doi.org/10.1021/cr900335q.Size.
[30] E. Ciotta, S. Paoloni, M. Richetta, P. Prosposito, P. Tagliatesta, C. Lorecchio, I. Venditti, I. Fratoddi, S. Casciardi, R. Pizzoferrato, Sensitivity to heavy-metal ions of unfolded fullerene quantum dots, Sensors (Switzerland). 17 (2017) 1–15, https://doi.org/10.3390/s17112614.
[31] V.N. Mehta, J.V. Rohit, S.K. Kailasa, Functionalization of silver nanoparticles with 5-sulfoanthranilic acid dithiocarbamate for selective colorimetric detection of Mn^{2+} and Cd^{2+} ions, New J. Chem. 40 (2016) 4566–4574, https://doi.org/10.1039/C5NJ03454J.
[32] P. Prosposito, F. Mochi, E. Ciotta, M. Casalboni, F. De Matteis, I. Venditti, L. Fontana, G. Testa, I. Fratoddi, Hydrophilic silver nanoparticles with tunable optical properties: application for the detection of heavy metals in water, Beilstein J. Nanotechnol. 7 (2016) 1654–1661, https://doi.org/10.3762/bjnano.7.157.
[33] D. Hu, Z. Sheng, P. Gong, P. Zhang, L. Cai, Highly selective fluorescent sensors for Hg 2 + based on bovine serum albumin-capped gold nanoclusters, Analyst 135 (2010) 1411–1416, https://doi.org/10.1039/c000589d.
[34] J. Xie, Y. Zheng, J.Y. Ying, Highly selective and ultrasensitive detection ofHg2+–Au+ interactions, Chem. Commun. (Camb.) 46 (2010) 961–963, https://doi.org/10.1039/B920748A.
[35] L. Shang, S. Dong, Silver nanocluster-based fluorescent sensors for sensitive detection of Cu(ii), J. Mater. Chem. 18 (2008) 4636–4640, https://doi.org/10.1039/b810409c.
[36] S. Roy, A. Baral, A. Banerjee, Tuning of silver cluster emission from blue to red using a bio-active peptide in water, ACS Appl. Mater. Interfaces 6 (2014) 4050–4056, https://doi.org/10.1021/am4055645.
[37] A. George, H. Gopalakrishnan, S. Mandal, Surfactant free platinum nanocluster as fluorescent probe for the selective detection of Fe (III) ions in aqueous medium, Sensors Actuators, B Chem. 243 (2017) 332–337, https://doi.org/10.1016/j.snb.2016.11.138.
[38] X. Hu, T. Liu, Y. Zhuang, W. Wang, Y. Li, W. Fan, Y. Huang, Recent advances in the analytical applications of copper nanoclusters, TrAC - Trends Anal. Chem. 77 (2016) 66–75, https://doi.org/10.1016/j.trac.2015.12.013.
[39] Y. Li, X. Hu, X. Zhang, H. Cao, Y. Huang, Unconventional application of gold nanoclusters/Zn-MOF composite for fluorescence turn-on sensitive detection of zinc ion, Anal. Chim. Acta 1024 (2018) 145–152, https://doi.org/10.1016/j.aca.2018.04.016.
[40] X. Hu, X. Liu, X. Zhang, H. Chai, Y. Huang, One-pot synthesis of the CuNCs/ZIF-8 nanocomposites for sensitively detecting H2O2 and screening of oxidase activity, Biosens. Bioelectron. 105 (2018) 65–70, https://doi.org/10.1016/j.bios.2018.01.019.
[41] B. Adhikari, A. Banerjee, Facile synthesis of water-soluble fluorescent silver nanoclusters and HgII sensing, Chem. Mater. 22 (2010) 4364–4371, https://doi.org/10.1021/cm1001253.
[42] Z. Sun, S. Li, Y. Jiang, Y. Qiao, L. Zhang, L. Xu, J. Liu, W. Qi, H. Wang, Silver nanoclusters with specific ion recognition modulated by ligand passivation toward fluorimetric and colorimetric copper analysis and biological imaging, Sci. Rep. 6 (2016) 1–9, https://doi.org/10.1038/srep20553.
[43] H. Xu, K.S. Suslick, Sonochemical synthesis of highly fluorescent Ag nanoclusters, ACS Nano 4 (2010) 3209–3214, https://doi.org/10.1021/nn100987k.
[44] M.A.H. Muhammed, F. Aldeek, G. Palui, L. Trapiella-Alfonso, H. Mattoussi, Growth of in situ functionalized luminescent silver nanoclusters by direct reduction and size focusing, ACS Nano 6 (2012) 8950–8961, https://doi.org/10.1021/nn302954n.
[45] S.A. Bogh, M.R. Carro-Temboury, C. Cerretani, S.M. Swasey, S.M. Copp, E.G. Gwinn, T. Vosch, Unusually large Stokes shift for a near-infrared emitting DNA-stabilized silver nanocluster, Methods Appl. Fluoresc. 6 (2018), https://doi.org/10.1088/2050-6120/aaa8bc.
[46] D. Schultz, E.G. Gwinn, Silver atom and strand numbers in fluorescent and dark Ag:DNAs, Chem. Commun. (Camb.) 48 (2012) 5748–5750, https://doi.org/10.1039/c2cc17675k.
[47] C.C. Huang, Z. Yang, K.H. Lee, H.T. Chang, Synthesis of highly fluorescent gold nanoparticles for sensing mercury(II), Angew. Chemie - Int. Ed. 46 (2007) 6824–6828, https://doi.org/10.1002/anie.200700803.
[48] L. Shang, S. Dong, Facile preparation of water-soluble fluorescent silver nanoclusters using a polyelectrolyte template, Chem. Commun. (Camb.) (2008) 1088–1090, https://doi.org/10.1039/b717728c.
[49] F. Lu, S. Zhou, J.J. Zhu, Photochemical synthesis of fluorescent Ag nanoclusters and enhanced fluorescence by ionic liquid, Int. J. Hydrogen Energy 38 (2013) 13055–13061, https://doi.org/10.1016/j.ijhydene.2013.03.081.
[50] S. Pietrantoni, R. Francini, R. Pizzoferrato, S. Penna, R. Paolesse, F. Mandoj, Energy transfer and excitation processes in thin films of rare-earth organic complexes for NIR emission, Phys. Status Solidi Curr. Top. Solid State Phys. 4 (2007) 1048–1051, https://doi.org/10.1002/pssc.200673853.
[51] D. Barettin, A. Di Carlo, R. De Angelis, M. Casalboni, P. Prosposito, Effect of dielectric Bragg grating nanostructuring on dye sensitized solar cells, Opt. Express 20 (2012) A888, https://doi.org/10.1364/OE.20.00A888.
[52] Z. Shen, H. Duan, H. Frey, Water-soluble fluorescent ag nanoclusters obtained from multiarm star poly(acrylic acid) as "molecular hydrogel" templates, Adv. Mater. 19 (2007) 349–352, https://doi.org/10.1002/adma.200601740.
[53] S. Navaladian, B. Viswanathan, T.K. Varadarajan, R.P. Viswanath, Fabrication of worm-like nanorods and ultrafine nanospheres of silver via solid-state photochemical decomposition, Nanoscale Res. Lett. 4 (2009) 471–479, https://doi.org/10.1007/s11671-009-9267-0.
[54] Y. He, Z. Du, H. Lv, Q. Jia, Z. Tang, X. Zheng, K. Zhang, F. Zhao, Green synthesis of silver nanoparticles by Chrysanthemum morifolium Ramat. extract and their application in clinical ultrasound gel, Int. J. Nanomedicine 8 (2013) 1809–1815, https://doi.org/10.2147/IJN.S43289.
[55] E. Ciotta, P. Prosposito, P. Tagliatesta, C. Lorecchio, L. Stella, S. Kaciulis, P. Soltani, E. Placidi, R. Pizzoferrato, Discriminating between different heavy metal ions with fullerene-derived nanoparticles, Sensors (Switzerland). 18 (2018) 1–15, https://doi.org/10.3390/s18051496.
[56] H. Wu, J. Liang, H. Han, A novel method for the determination of Pb2+ based on the quenching of the fluorescence of CdTe quantum dots, Microchim. Acta. 161 (2008) 81–86, https://doi.org/10.1007/s00604-007-0801-4.
[57] Y. Wen, C. Peng, D. Li, L. Zhuo, S. He, L. Wang, Q. Huang, Q.H. Xu, C. Fan, Metal ion-modulated graphene-DNAzyme interactions: Design of a nanoprobe for fluorescent detection of lead(II) ions with high sensitivity, selectivity and tunable dynamic range, Chem. Commun. (Camb.) 47 (2011) 6278–6280, https://doi.org/10.1039/c1cc11486g.
[58] S. Naaz, P. Chowdhury, Sunlight and ultrasound-assisted synthesis of photoluminescent silver nanoclusters: a unique 'knock out' sensor for thiophilic metal ions, Sensors Actuators, B Chem. 241 (2017) 840–848, https://doi.org/10.1016/j.snb.2016.10.116.
[59] B. Zhang, C. Wei, Highly sensitive and selective detection of Pb2+ using a turn-on fluorescent aptamer DNA silver nanoclusters sensor, Talanta 182 (2018) 125–130,

https://doi.org/10.1016/j.talanta.2018.01.061.
[60] J. Wang, Z. Zhang, X. Gao, X. Lin, Y. Liu, S. Wang, A single fluorophore ratiometric nanosensor based on dual-emission DNA-templated silver nanoclusters for ultra-sensitive and selective Pb2+ detection, Sensors Actuators, B Chem. 282 (2019) 712–718, https://doi.org/10.1016/j.snb.2018.11.121.
[61] C. Wang, H. Cheng, Y. Sun, Z. Xu, H. Lin, Q. Lin, C. Zhang, Nanoclusters prepared from a silver/gold alloy as a fluorescent probe for selective and sensitive determination of lead(II), Microchim. Acta. 182 (2015) 695–701, https://doi.org/10.1007/s00604-014-1375-6.
[62] M. Ganguly, C. Mondal, J. Jana, A. Pal, T. Pal, Photoproduced fluorescent Au(I)@(Ag 2 /Ag 3)-Thiolate giant cluster: an intriguing sensing platform for DMSO and Pb(II), Langmuir 30 (2014) 348–357, https://doi.org/10.1021/la403848z.
[63] J.F. Moulder, W.F. Stickle, P.E. Sobol, K.D. Bomben, Handbook of X-Ray Photoelectron Spectroscopy, Eden Prairie, Minnesota, U.S.A, 1995.
[64] I. Lopez-Salido, D.C. Lim, Y.D. Kim, Ag nanoparticles on highly ordered pyrolytic graphite (HOPG) surfaces studied using STM and XPS, Surf. Sci. 588 (2005) 6–18, https://doi.org/10.1016/j.susc.2005.05.021.
[65] V. Ambrogi, A. Donnadio, D. Pietrella, L. Latterini, F.A. Proietti, F. Marmottini, G. Padeletti, S. Kaciulis, S. Giovagnoli, M. Ricci, Chitosan films containing mesoporous SBA-15 supported silver nanoparticles for wound dressing, J. Mater. Chem. B Mater. Biol. Med. 2 (2014) 6054, https://doi.org/10.1039/C4TB00927D.
[66] B. Heidelberg New York Barcelona Hong Kong London Milan Paris Tokyo Bernard Valeur, J.-C. Brochon Eds, Springer New Trends in Fluorescence Spectroscopy Applications to Chemical and Life Sciences, n.d.
[67] B. Valeur, Design principles of fluorescent molecular sensors for cation recognition, Coord. Chem. Rev. 205 (2000) 3–40, https://doi.org/10.1016/S0010-8545(00)00246-0.
[68] S.K. Kim, S.H. Lee, J.Y. Lee, J.Y. Lee, R.A. Bartsch, J.S. Kim, An Excimer-Based, Binuclear, On - Off Switchable Calix [4] crown Chemosensor, J. Am. Chem. Soc. 126 (2004) 16499–16506, https://doi.org/10.1021/jo200650f.
[69] A.T. Afaneh, G. Schreckenbach, Fluorescence Enhancement/Quenching based on metal orbital control: computational studies of a 6-Thienyllumazine-Based mercury sensor, J. Phys. Chem. A 119 (2015) 8106–8116, https://doi.org/10.1021/acs.jpca.5b04691.